Semnan University

Journal of Modeling & Simulation in Electrical & Electronics Engineering (MSEEE)

Journal homepage: **https://mseee.semnan.ac.ir/**

ISSN: 2821-0786

Comparative Thermal Loss Analysis of a Dual Active Bridge Converter With and Without LLL Resonant Tank for EV Charger Applications

Amir Hossein Najaei[1]* and Naser Eskandarian[1]

***Abstract*—Dual Active Bridge (DAB) DC–DC converters are commonly used in high-power isolated systems, including on-board and off-board electric vehicle chargers, because of their inherent bidirectional power transfer capability and compact design. However, as charging power levels and efficiency targets continue to rise in modern EV infrastructures, the associated increase in semiconductor losses and device temperatures makes thermal performance a critical design concern. Despite the advantages, traditional DAB converters with single-phase shift (SPS) control tend to incur considerable switching losses, especially at high power levels, which can raise semiconductor junction temperatures. In particular, the lack of a detailed, application-oriented comparison between the thermal loss behavior of conventional DAB converters and resonant-assisted variants under realistic EV charging conditions limits designers' ability to select the most thermally efficient topology. For this reason, the power-loss characteristics and thermal response of a conventional DAB converter, related to its switches, are evaluated and compared with those of an LLL-tank-assisted DAB topology. The two converter topologies are modeled in MATLAB/Simulink and PLECS and tested under identical operating conditions, including power level and control method, so that the results can be directly compared. Semiconductor losses are then estimated by considering both conduction and switching components, with switching energy values taken from the IGBT manufacturer's datasheet. Junction temperature is then estimated through a steady-state thermal resistance model that relates total power dissipation to ambient conditions. The influence of the LLL resonant tank on converter current profiles and thermal stress is analyzed. Simulation results show that introducing the LLL resonant tank reduces switching and conduction losses, thereby lowering the junction temperature of the power semiconductor devices compared with the conventional DAB converter. This improvement is achieved without altering the original SPS control approach. The outcomes of this work offer valuable guidance for thermally optimized design of high-power isolated DC–DC converters used in electric vehicle charging systems, bridging an important gap between efficiency-oriented analysis and comprehensive thermal loss evaluation for practical EV charger applications.**

This work presents a systematic comparative thermal loss analysis of a Dual Active Bridge (DAB) converter operating with and without an LLL resonant tank, specifically for high-power EV charger applications. Unlike prior studies that primarily focus on efficiency enhancement or soft-switching performance of resonant-assisted DAB topologies, this study provides a detailed device-level evaluation of thermal and loss distribution under identical operating conditions. The proposed comparison framework quantifies conduction and switching losses and the resulting impact on system-level thermal management requirements. This approach enables a clearer understanding of the trade-offs between conventional DAB and LLL-assisted configurations in terms of efficiency, thermal performance, and practical constraints for EV charger implementation.

***Index Terms*- Dual Active Bridge Converter, LLL Resonant Tank, Switching Loss Analysis, Thermal Modeling, Junction Temperature, Electric Vehicle Chargers.**

I. INTRODUCTION

As electric vehicle (EV) adoption continues to expand worldwide, the demand for efficient, reliable, and compact power conversion systems in both on-board and off-board charging infrastructures has increased significantly. High-

Received: 2026-02-16 Revised: 2026-05-09 Accepted: 2026-06-07
1. Faculty of Electrical and Computer Engineering, Semnan University, Semnan, Iran.
*Corresponding author Email: amirhosseinnajaei@semnan.ac.ir

Cite this article as:
Najaei, A. H.; and Eskandarian, N. (2026). Comparative Thermal Loss Analysis of a Dual Active Bridge Converter With and Without LLL Resonant Tank for EV Charger Applications. *Journal of Modeling & Simulation in Electrical & Electronics Engineering (MSEEE). Semnan University Press . 6 (4), 11-19.*
DOI: https://doi.org/10.22075/mseee.2026.40617.1254

© 2026 The Author(s). Journal of Modeling & Simulation in Electrical & Electronics Engineering is published by Semnan University Press. This is an open-access article under the CC-BY 4.0 license. (https://creativecommons.org/licenses/by/4.0/)

power EV chargers require galvanically isolated DC–DC conversion stages to ensure safety, enable voltage level adaptation, and support bidirectional power flow for vehicle-to-grid (V2G) operation. Among various isolated DC–DC converter topologies, the Dual Active Bridge (DAB) converter has emerged as a widely adopted solution due to its symmetrical structure, inherent bidirectional capability, high power density, and suitability for high-frequency transformer-based isolation [1]-[4].

The conventional DAB converter typically operates under Single Phase Shift (SPS) modulation, where the transferred power is controlled by the relative phase shift between the primary and secondary full-bridge voltages. While SPS control offers simplicity and robustness, it is well documented that conventional DAB converters can suffer from excessive circulating currents, hard-switching behavior, and elevated current stress under high power transfer, wide voltage conversion ratios, and light-load operating conditions [2], [3], [5], [6]. These effects lead to increased conduction and switching losses in power semiconductor devices, resulting in higher junction temperatures and reduced system efficiency. In EV charging applications, where converters often operate continuously at high power levels, thermal stress becomes a dominant design constraint affecting reliability, lifetime, and cooling system requirements [7], [8].

To mitigate these drawbacks, a substantial body of research has focused on improving DAB performance through advanced modulation strategies. Techniques such as dual-phase-shift (DPS), triple-phase-shift (TPS), and extended phase-shift (EPS) control have been proposed to reduce circulating current, improve soft-switching conditions, and enhance efficiency across a wider operating range [1],[2],[9],[10]–[12]. Although effective, these modulation schemes typically increase control complexity, computational burden, and sensitivity to parameter variations, which may limit their practicality in industrial EV charging systems where robustness and simplicity are highly valued [13],[14].

An alternative approach to performance improvement involves modifying the DAB power stage itself by integrating resonant or quasi-resonant networks. Resonant-assisted DAB topologies, including CLLC, LCL, and other multi-element resonant structures, have been investigated to reshape current waveforms, reduce di/dt during switching transitions, and extend zero-voltage-switching (ZVS) operation [15–18]. These topologies leverage interactions between transformer leakage inductance and additional resonant elements to soften switching transitions and reduce switching energy losses without fundamentally altering the bidirectional nature of the DAB converter.

Among resonant-assisted structures, LLL-type resonant tanks have attracted attention for their ability to improve switching behavior while maintaining compatibility with conventional SPS control [19]-[21]. By introducing multiple inductive elements into the power transfer path, the LLL resonant tank can modify current dynamics during commutation intervals, reduce instantaneous voltage–current overlap in switching devices, and alleviate current stress. This makes LLL-assisted DAB converters particularly attractive for high-power applications where switching frequency and device ratings impose strict thermal constraints.

Despite the extensive literature on efficiency optimization and soft-switching operation of resonant and quasi-resonant DAB converters, relatively few studies have explicitly examined the thermal implications of these topological modifications. In high-power EV charging systems, semiconductor junction temperature is a critical performance metric, as it directly influences device reliability, cooling system design, and long-term operational stability [6],[8],[22],[23]. While several works report reductions in electrical losses, they often do not quantify how these reductions translate into junction temperature improvement under identical operating and thermal boundary conditions [24],[25]. As a result, the thermal benefits of resonant-assisted DAB converters remain insufficiently characterized.

Thermal modeling of power electronic converters is therefore essential for meaningful performance evaluation. Datasheet-based loss estimation combined with steady-state thermal resistance networks is widely used in comparative studies to relate semiconductor power dissipation to junction temperature rise [22], [26]-[28]. Such approaches provide valuable insight into the coupling between electrical loss mechanisms and thermal stress while maintaining reasonable modeling complexity, making them suitable for early-stage design evaluation and topology comparison.

Motivated by these considerations, this paper presents a comparative thermal and power loss analysis of a conventional SPS-controlled DAB converter and a DAB converter assisted by an LLL resonant tank. Both topologies are modeled in MATLAB/Simulink and PLECS and evaluated under identical electrical operating conditions, power rating, switching frequency, and control strategy to ensure a fair and topology-independent comparison. Semiconductor conduction and switching losses are estimated using datasheet-based models, and a steady-state thermal resistance network is employed to calculate junction temperature. By analyzing current waveforms, loss components, and resulting thermal behavior, this study aims to clarify the impact of LLL resonant tank integration on the thermal performance of DAB converters used in EV charging applications.

II. Converter Topology Under Study

This work compares two isolated bidirectional DC–DC converter topologies derived from the Dual Active Bridge (DAB) family: (A) a conventional soft-switched DAB operating under Single Phase Shift (SPS) control, and (B) a DAB augmented by a LLL resonant tank (LLL-DAB) while retaining the same SPS control scheme. Both topologies are modeled and simulated under identical electrical and control conditions to permit direct comparison of electrical losses and thermal response. The following subsections define each topology, enumerate modeling assumptions, and list the key parameters used for fair comparison.

A. Conventional Dual Active Bridge Converter

The conventional DAB under study consists of two full-bridge H-bridge converters (primary and secondary) connected by a high-frequency isolated transformer, as illustrated in Fig. 1. Each H-bridge converts its DC link voltage into a bipolar square-wave voltage applied to the transformer. Power transfer is controlled by the relative phase shift $\Delta\varphi$ between the primary and secondary bridge waveforms (SPS modulation) [1],[3].

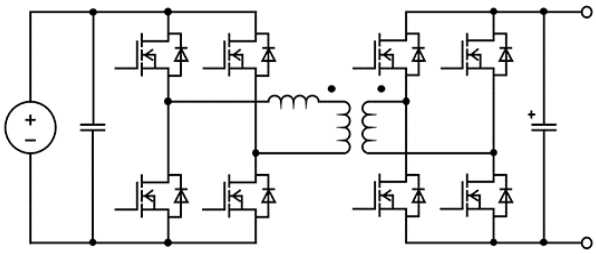

Fig. 1. Overall Topology of a conventional Dual Active Bridge Converter (DABC).

The transformer leakage inductance $L\ell$ and any intentionally inserted series inductance limit the current slope and determine the energy exchange during each switching interval. Key characteristics and modeling choices for the conventional DAB are:

- Topology: two H-bridges + high-frequency transformer with leakage inductance $L\ell$.
- Modulation: Single Phase Shift (SPS) — phase shift $\Delta\varphi$ controls the average power flow while switching frequency fs is fixed.
- Dominant reactive element: series leakage inductance $L\ell$.
- Assumptions: ideal transformer turns ratio n, lossless magnetics except for leakage $L\ell$, H-bridge switches represented by datasheet-based (Infineon IKQ50N120CH3) switching and conduction models in the loss calculation stage (detailed in Section III) [25]. Parasitic capacitances and stray resistances are included in device-level loss estimation but are not treated as separate tuning elements in the baseline topology.

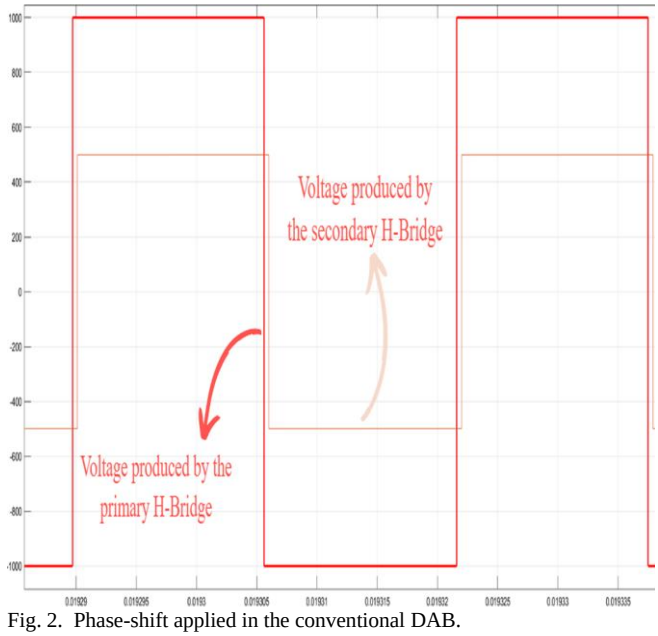

Fig. 2. Phase-shift applied in the conventional DAB.

Fig. 2 illustrates the distinct phase-shift between the voltages generated by each H-bridge. As shown, both the conventional Dual Active Bridge (DAB) and the LLL-DAB converter are designed to facilitate a DC-DC conversion from 1000 V to 500 V. Furthermore, the series inductance of the high-frequency (HF) transformer is a critical parameter in the system model. A value of 0.0102 mH is utilized for both the conventional DAB and LLL-DAB configurations to accurately characterize their power transfer behavior. To facilitate the understanding of the operating behavior of a conventional Dual Active Bridge converter, the voltage across the leakage inductance and the corresponding leakage inductance current waveforms are illustrated in Fig. 3. In addition, the battery state of charge (SOC) and the converter output voltage are presented in Fig. 4.

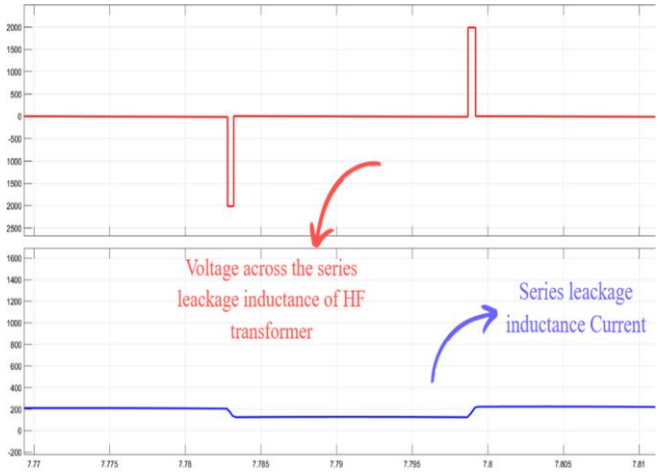

Fig. 3. Voltage and current of the leakage inductance in the conventional DAB.

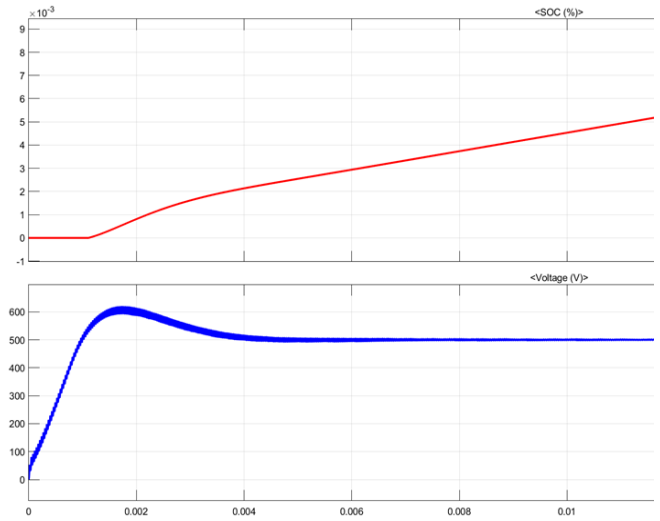

Fig. 4. SOC and Output Voltage of the conventional DAB.

B. LLL Resonant Tank DAB Converter

The LLL-DAB topology retains the same H-bridges and isolated transformer as the conventional DAB. Still, it introduces a passive resonant network (here referred to as an LLL resonant tank) that interacts with the transformer leakage inductance and device parasitic capacitances to alter switching transients and waveform shapes. The resonant network is arranged so that, during switching transitions, the current of the switching device are reshaped to reduce the instantaneous overlap of voltage and current and thereby reduce switching energy per transition as the topology illustrated in Fig. 5. The resonant network is arranged so that, during switching transitions, the current of the switching device is reshaped to reduce the instantaneous overlap of voltage and current and thereby reduce switching energy per transition [9],[19].

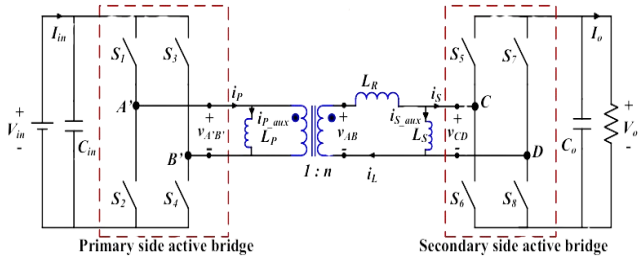

Fig. 5. Overall Topology of an LLL-DAB Converter.

Important aspects of the LLL-tank arrangement used in this study are:

- Resonant network: the LLL tank comprises three inductive elements arranged to form a resonant path that couples to the transformer leakage inductance and device capacitances. The practical implementation in the Simulink model uses discrete inductors L1, L2, and L3, whose values are just to establish a target resonance that produces favorable current shaping at switching instants.

- Placement and interaction: The resonant tank is inserted between the H-bridges and the transformer on both the primary and secondary sides, enabling resonant current flow through the transformer leakage inductance during commutation intervals. The conventional power transfer path is preserved for steady-state operation, while the resonant branch handles transient energy exchange.

- Control compatibility: SPS modulation is preserved for power control; no additional active timing or phase-interleaving control is required, and it is considered a simple modulation method. The resonant tank is passive and does not alter the steady-state phase-shift control law; thus, the two topologies are compared under identical control inputs (same $\Delta\varphi$ and fs).

- Design objective: We use L1=L2=L3=0.0102 mH values only to show the effect of the LLL resonant tank in this paper, as this paper is only a comparative study.

- Expected switching behavior: softening of transitions, reduced di/dt at switching instants, and altered current waveform shape; representative waveforms for the LLL-DAB are shown.

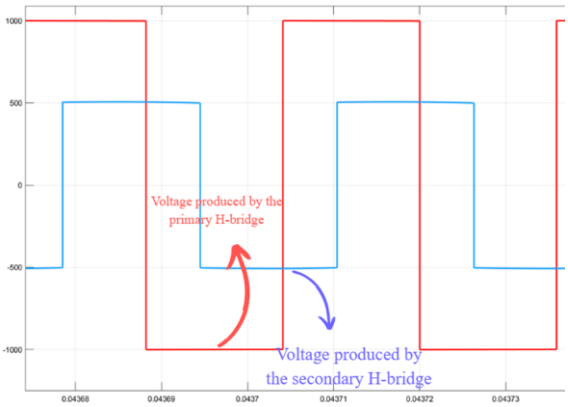

Fig. 6. Phase-shift applied in the LLL-DAB.

As is shown, the difference between Figs. 2 and 6 is obvious.

Moreover, the phase shift in Fig. 6 is much more than that in Fig. 2.

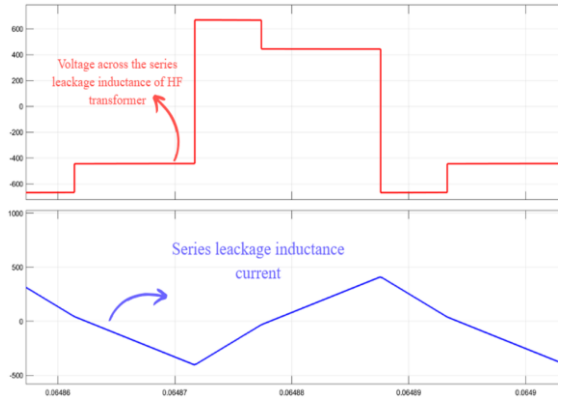

Fig. 7. Voltage and current of the leakage inductance in the LLL-DAB.

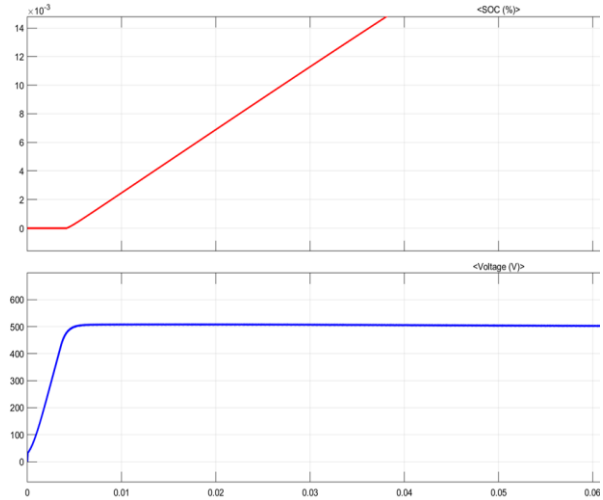

Fig. 8. SOC and Output Voltage of the LLL-DAB.

The leakage inductance voltage and current waveforms of the LLL-DAB converter are shown in Fig. 7, while the battery SOC and output voltage are presented in Fig. 8.

III. Semiconductor Power Loss Modeling

This section describes the device-level loss model used to estimate semiconductor dissipation in both converter topologies. The model is datasheet-driven, theoretical, and implemented in PLECS, so that switching and conduction losses are computed from device-level waveforms and the manufacturer's different variables curves [27].

A. Switching Loss Model

The structure and architecture of a DAB consist of two full bridges, and each bridge consists of four switches. Therefore, the total switching losses of our converter equal the algebraic sum of the switching losses of our eight switches in the converter.

$$P_{sw} = \sum_{i=1}^{8} (\frac{1}{2}) V_{sw} I_{sw} (t_{on} + t_{off}) f_{sw} \quad (1)$$

Where Vsw and Isw are the voltage and current through the switch during its on and off states, as clearly stated in each switch datasheet [27].

Also, by including explicit dependence on device voltage/current at switching instants, the two bridges can be interpreted as:

$$P_{sw,k} = f_{sw}(E_{on,k} + E_{off,k}) \quad (2)$$

Where fsw is the switching frequency and Eon, and Eoff are the energy lost in device k during turn-on switching and the

energy lost in device k during turn-off switching r. For a deeper dive, we have the following equations for Eon and Eoff:

$$E_{on,k} \approx \int v_{ds,k}(t)\, i_{d,k}(t).\, dt \quad during\ on\ time \qquad (3)$$

$$E_{off,k} \approx \int v_{ds,k}(t)\, i_{d,k}(t).\, dt \quad during\ off\ time \qquad (4)$$

For simplification in switching loss calculation, we have to consider some assumptions: first, the current through the Core resistance Rm and magnetizing inductor is negligible, as these currents are much less than the series inductance Leq and Req. As a result, we should precisely calculate the overall switching losses based on the given equation.

B. Conduction Loss Model

Conduction loss is evaluated from device conduction characteristics and the actual current waveform. The model is selected based on device type and available datasheet parameters.

The exact instantaneous conduction power is

$$P_{cond}(t) = V_{ce} i_c(t) \qquad (5)$$

Where Vce is the voltage across the switch, and ic is actually the current passing through it.

And the average conduction power over one switching period is

$$P_{cond} = \left(\frac{1}{T_s}\right) \int_{t0}^{t0+Ts} V_{ce}(t).\, i_c(t).\, dt \qquad (6)$$

For approximation, we would have:

$$V_{ce}(t) = V_f\ sign(i_c(t)) + R_{on}\ {I^2}_{rms} \qquad (7)$$

then:

$$I_{rms} = \sqrt{\frac{1}{T_s} \int_{t0}^{t0+Ts} {i_c}^2(t).\, dt} \qquad (8)$$

When waveform integration is impractical, we can use a relevant datasheet parameter for the switch we are analyzing.

C. Total Device Power Loss

The total steady-state power dissipated by a semiconductor device is the sum of conduction and switching losses. For each power device, we compute:

$$P_{loss} = P_{cond} + P_{sw} \qquad (9)$$

Where P_{loss} is the total power loss of the switch, P_{cond} is the conduction power loss of the switch, and P_{sw} is the switching power loss of the switch.

For a bridge composed of N identical switching devices and M diodes, the bridge loss is

$$P_{bridge} = \sum_{i=1}^{N} P_{loss,switchi} + \sum_{j=1}^{M} P_{loss,diodej} \qquad (10)$$

IV. Thermal Modeling and Junction Temperature Estimation

Electrical loss reduction is only meaningful in high-power converter design if it translates into reduced thermal stress on semiconductor devices. For this reason, the power losses calculated in Section III are used as inputs to a device-level thermal model to estimate junction temperature under steady-state operating conditions. This section describes the adopted thermal modeling approach, assumptions, and junction temperature calculation methodology used for both converter topologies.

A. Thermal Modeling Approach

A lumped, steady-state thermal resistance model is employed to estimate the junction temperature of power semiconductor devices [7],[27]. This approach is widely used in preliminary thermal design and comparative studies, as it provides a direct and physically meaningful relationship between device power dissipation and temperature rise while avoiding excessive computational complexity.

Each semiconductor device is represented by a one-dimensional thermal network consisting of:

- Junction-to-case thermal resistance Rth(j-c), obtained from the manufacturer's datasheet.
- Junction-to-case thermal resistance Rth(j-c), obtained from the manufacturer's datasheet.

The thermal model assumes uniform heat generation within the semiconductor die and neglects lateral thermal coupling between devices. This assumption is reasonable for the comparative analysis performed in this work, as identical thermal boundary conditions are applied to both converter topologies.

B. Junction Temperature Calculation

Under steady-state conditions, the junction temperature T_j of each device is calculated from the total device power loss using the linear thermal resistance relationship.

$$T_j = T_{amb} + P_{loss}(R_{th(j-c)} + R_{th(c-a)}) \qquad (11)$$

Where

- Tamb is the ambient temperature.
- Ploss is the total steady-state power dissipation of the device calculated in Section III.
- Rth(j-c) is the junction-to-case thermal resistance.
- Rth(c-a) is the case-to-ambient thermal resistance.

The junction temperature is evaluated individually for the targeted switching device in the converter.

V. Results and Comparison

This section presents and compares the simulation results obtained for the conventional DAB converter and the LLL-tank-assisted DAB under identical electrical, modulation (SPS), ambient temperature, and cooling conditions [29].

Fig. 9(a) and Fig. 9(b) show the detailed Simulink simulation models of the conventional DAB converter and the proposed LLL-resonant-tank-assisted DAB, respectively.

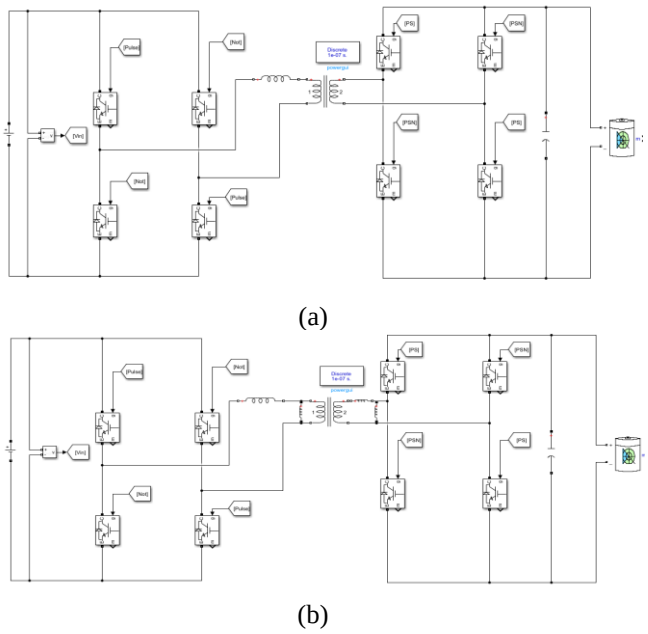

(a)

(b)

Fig. 9. Simulink model of (a) Conventional DAB and (b) LLL-DAB

The performance metrics considered in this comparison include:

- Switching loss for the switch
- Conduction loss for the switch
- Total semiconductor power loss
- Peak junction temperature
- Thermal distribution across the active switch

All results are extracted after steady-state operation is reached to ensure consistency and repeatability.

A. Switching Loss Comparison

Switching losses are calculated using the PLECS thermal model detailed in Section III-A. The switching loss comparison indicates that the LLL-assisted DAB achieves substantially less switching dissipation than the conventional topology. As summarized in Table I, the total switching loss of the LLL-DAB is reduced by approximately 292 W relative to the conventional DAB.

TABLE I
Estimated Switching Loss Results

Topology	Estimated Switching Loss
DAB	302.1 W
LLL-DAB	9.54 W

This reduction is mainly attributed to the resonant current shaping introduced by the LLL tank. In the conventional DAB, the bridge current overlaps more significantly with voltage transitions during commutation, resulting in higher turn-on and turn-off energy losses. By contrast, the LLL network modifies the current waveform so that the current magnitude at switching instants is reduced, which improves the soft-switching condition and limits the simultaneous presence of high voltage and current.

The switching loss reduction can therefore be interpreted as:

$$\Delta P_{sw} = P_{sw,conv} - P_{sw,LLL} \tag{12}$$

B. Conduction Loss Comparison

Conduction losses for both converters are also calculated using PLECS. Table II summarizes the conduction loss results.

TABLE II
Estimated Conduction Losses Results

Topology	Estimated Conduction Loss
DAB	131.12 W
LLL-DAB	9.12 W

A significant discrepancy is observed between the switch conduction losses of each topology. The LLL-DAB demonstrates a reduction of approximately 122W relative to the conventional DAB configuration.

This reduction can be explained by the altered current RMS profile resulting from the resonant tank integration. The LLL network reshapes the circulating current and reduces peak current stress, which directly lowers RMS current through the semiconductor devices. Since conduction losses are proportional to the following term

$$P_{cond} \propto {I^2}_{rms}.R_{on} \tag{13}$$

Even a moderate reduction in RMS current leads to a noticeable decrease in conduction dissipation.

The conduction-loss improvement can be written as:

$$\Delta P_{cond} = P_{cond,conv} - P_{cond,LLL} \tag{14}$$

C. Total Power Loss Comparison

As mentioned, the combined effect of switching and conduction losses leads to the total power loss of the switch.

Combining the reported reductions in switching and conduction losses, the LLL-DAB achieves a significantly lower total power loss than the conventional DAB. This reduction is particularly important because the junction temperature rises approximately linearly with total dissipated power under steady-state thermal conditions:

$$\Delta T_j = P_{loss} - R_{\theta ja} \tag{15}$$

Therefore, the reduction in total semiconductor loss directly translates into lower thermal loading, reduced heat sink demand, and improved converter reliability.

D. Junction Temperature Comparison

Table III and Fig. 10 show that the conventional DAB exhibits a noticeably higher junction temperature than the LLL-DAB under the same ambient temperature and cooling conditions. The LLL-assisted topology reduces the peak junction temperature by approximately 24°C, representing a substantial improvement in reliability.

This behavior follows directly from (11). Because LLL-DAB switches dissipate less total loss, the device temperature rise above ambient is correspondingly smaller. More importantly, the thermal distribution is also improved. In conventional DAB, thermal stress is concentrated more heavily on the primary-side devices due to higher circulating current and greater current overlap during switching. This concentration leads to localized hot spots and may accelerate thermo-mechanical fatigue.

In contrast, the LLL-DAB exhibits a more uniform thermal profile across the active switches. The thermal balance improves because the resonant tank redistributes current flow

and reduces peak current stress. As a result, the temperature difference among devices becomes smaller, which is highly beneficial for long-term reliability in EV charger applications.

The thermal improvement may be summarized as:

$$\Delta T_j = T_{j,conv} - T_{j,LLL} \quad (16)$$

The observed reduction in junction temperature confirms that the improved electrical performance of the LLL tank directly enhances thermal performance.

TABLE III
Estimated Junction Temperature Results

Topology	Estimated Junctions Temperatures
DAB	54.1 °C
LLL-DAB	30.06 °C

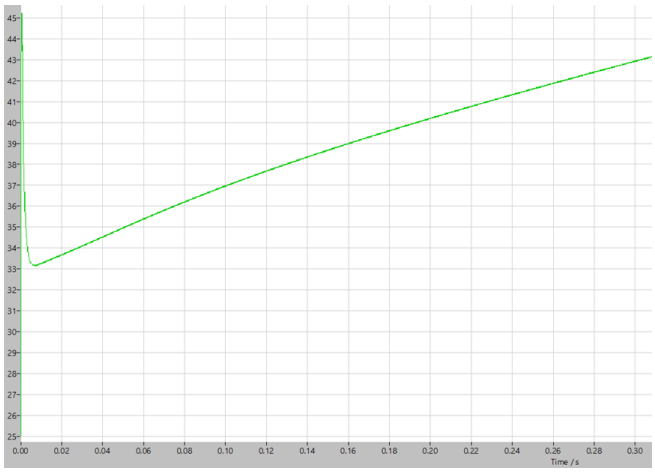

(a)

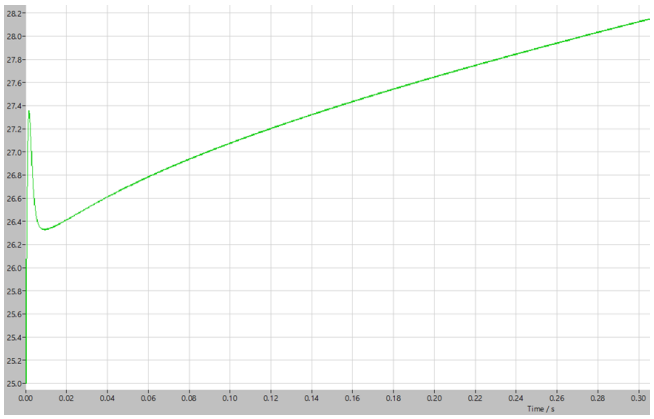

(b)

Fig. 10. Estimated junction temperature of the switch in (a) Conventional DAB, (b) LLL-DAB

E. Discussion of Thermal Distribution

Beyond peak temperature, the spatial thermal distribution is an essential indicator of converter robustness. In conventional DAB, the higher RMS and commutation current cause stronger thermal stress on selected switches, particularly those operating under more severe current-overlap conditions. This results in a non-uniform temperature field and localized hot spots. By contrast, the LLL topology reduces this non-uniformity through resonant current shaping. Lower current stress diminishes the thermal load on the most critical devices and spreads dissipation more evenly across the bridge. This balanced thermal distribution is desirable because:

1. It reduces hotspot severity,
2. It lowers the likelihood of bond-wire and solder fatigue,
3. It improves long-term reliability under repetitive charging cycles,
4. It relaxes cooling-system requirements.

Therefore, the advantage of the LLL-DAB is not limited to lower losses; it also includes better thermal symmetry and more favorable reliability behavior.

F. Critical Evaluation

Although the LLL tank improves both electrical and thermal performance, it introduces additional passive components and design sensitivity. The resonant parameters must be carefully selected to preserve the soft-switching region and avoid performance degradation under parameter drift. Moreover, the increased component count may raise cost and design complexity. Nevertheless, for high-power EV charger applications where efficiency, thermal stability, and reliability are more important than minimal hardware count, the LLL-assisted DAB offers a compelling advantage. The reduction in switching and conduction losses, and in junction temperature, provides strong evidence that resonant tank integration is an effective approach for improving converter thermal performance.

The overall Comparison of the two converter topologies is summarized in Table IV. Table IV provides an easy-to-use comparison of the main electrical and thermal performance metrics. The results clearly indicate that integrating the LLL resonant tank significantly improves the converter's thermal and electrical performance by reducing switching and conduction losses, leading to lower junction temperatures and improved thermal balance among semiconductor devices. However, design constraints should be considered.

TABLE IV
Overall Comparison between DAB & LLL-DAB

Performance Metric	Conventional DAB	LLL-DAB
Switching Loss	Higher	Lower
Conduction Loss	Higher	Lower
Total Semiconductor Loss	Higher	Lower
Peak Junction Temperature	Higher	Lower
Number of Elements	Lower	Higher
Design Complexity	Lower	Higher
Control Complexity	Lower	Higher

VI. CONCLUSION

This paper presents a comparative thermal and power-loss analysis of a conventional dual-active-bridge (DAB) converter and an LLL-tank-assisted DAB topology for high-power isolated DC–DC applications, such as EV charging systems. Detailed switching and conduction loss models were developed and implemented under identical operating conditions to ensure a fair and topology-independent comparison. A lumped thermal resistance network was then employed to estimate semiconductor junction temperatures based on the calculated device power dissipation.

Thermal analysis confirms that the reduction in junction temperature closely follows the trend in loss reduction, highlighting the strong coupling between electrical loss mechanisms and thermal performance. Lower junction temperatures imply improved semiconductor reliability, relaxed cooling requirements, and potentially higher allowable power density, all of which are critical factors in compact and high-efficiency EV charger designs.

Overall, the findings indicate that resonant-assisted DAB converters offer tangible thermal advantages beyond efficiency improvement alone. These results support the suitability of LLL-tank-assisted DAB topologies for next-generation high-power DC fast-charging systems where thermal constraints and long-term reliability are of primary concern.

Finally, this paper contributes to the existing literature by providing a structured, quantitative thermal-loss-oriented comparison between conventional DAB and LLL-resonant-assisted DAB topologies under realistic EV charger operating conditions. The present study distinguishes itself by performing a detailed breakdown of conduction and switching losses at the semiconductor device level. The results demonstrate that adding the LLL resonant tank alters not only the switching dynamics but also the thermal loading profile, which has important implications for reliability, cooling design, and long-term EV charger operation.

ACKNOWLEDGMENT

The authors thank the Power Electronics Research group at Semnan University for their academic support, guidance, and constructive feedback during this research. The authors would like to acknowledge the use of MATLAB/ Simulink and PLECS for the modeling and simulation work presented in this paper.

CONFLICTS OF INTEREST

The authors declare that there is no conflict of interest regarding the publication of this article.

AI DISCLOSURE

The authors used ChatGPT (OpenAI, San Francisco, USA) to assist in language editing and improving the clarity of the manuscript. All AI-assisted outputs were reviewed and verified by the authors.

DATA AVAILABILITY

All data generated or analyzed during this study are included in this published article.

FUNDING STATEMENT

This research received no specific grant from any funding agency in the public, commercial, or not-for-profit sectors.

AUTHORS' CONTRIBUTIONS

The authors have contributed to the whole research and preparation of the manuscript.

REFERENCES

[1] J. He, Y. Chen, J. Lin, J. Chen, L. Cheng, and Y. Wang, "Review of modeling, modulation, and control strategies for the dual-active-bridge DC/DC converter," *Energies*, vol. 16, no. 18, Art. no. 6646, 2023.

[2] L. Shao, Z. Shan, F. Gao, H. Chen, D. Sha, and T. Dragicevic, "Modeling and advanced control of dual-active-bridge DC–DC converters: A review," *IEEE Trans. Power Electron.*, vol. 37, no. 2, pp. 1524–1547, Feb. 2022.

[3] R. W. De Doncker, D. M. Divan, and M. H. Kheraluwala, "A three-phase soft-switched high-power-density DC/DC converter for high-power applications," *IEEE Trans. Ind. Appl.*, vol. 27, no. 1, pp. 63–73, Jan. 1991.

[4] M. M. R. S. M. H. Alam, F. A. Rafi, S. B. Deb, et al., "Comprehensive review on the charging technologies of electric vehicles (EV) and their impact on power grid," *IEEE Access*, 2025.

[5] H. Qin and J. W. Kimball, "Generalized average modeling of dual active bridge DC–DC converter," *IEEE Trans. Power Electron.*, vol. 27, no. 4, pp. 2078–2084, Apr. 2012.

[6] M. R. Farid, A. L. Elrefai, and S. M. Abdelkader, "Comparative analysis of single phase shift and extended phase shift modulations in dual active bridge converters for EV fast chargers," *Renew. Energy Power Qual. J.*, 2026.

[7] M. Ciappa, "Selected failure mechanisms of modern power modules," *Microelectron. Reliab.*, vol. 42, no. 4–5, pp. 653–667, 2002.

[8] A. Castellazzi, A. Fayyaz, G. Romano, L. Yang, M. Riccio, and A. Irace, "SiC power MOSFETs performance, robustness, and technology maturity," *IEEE J. Emerg. Sel. Topics Power Electron.*, vol. 4, no. 3, pp. 803–815, Sep. 2016.

[9] J. Everts, "Closed-form solution for efficient ZVS modulation of DAB converters," *IEEE Trans. Power Electron.*, vol. 32, no. 10, pp. 7561–7576, Oct. 2017.

[10] S. Inoue and H. Akagi, "A bidirectional DC–DC converter for an energy storage system with galvanic isolation," *IEEE Trans. Power Electron.*, vol. 22, no. 6, pp. 2299–2306, Nov. 2007.

[11] B. Zhao, Q. Song, W. Liu, and Y. Sun, "Overview of dual-active-bridge isolated bidirectional DC–DC converter and its current control strategies," *IEEE Trans. Power Electron.*, vol. 29, no. 8, pp. 4091–4106, Aug. 2014.

[12] F. Krismer and J. W. Kolar, "Efficiency-optimized high-current dual active bridge converter for automotive applications," *IEEE Trans. Ind. Electron.*, vol. 59, no. 7, pp. 2745–2760, Jul. 2012.

[13] T. Younis, F. S. Al-Ismail, S. M. Amrr, and S. M. Suhail Hussain, "Optimization strategies for triple-phase-shift modulation in dual-active-bridge converters: A comprehensive review," *IEEE Access*, 2025.

[14] J. He, Y. Chen, J. Lin, J. Chen, L. Cheng, and Y. Wang, "Review of modeling, modulation, and control strategies for the dual-active-bridge DC/DC converter," *Energies*, 2023.

[15] R. Beiranvand, B. Rashidian, M. R. Zolghadri, and S. M. H. Alavi, "A design procedure for optimizing the LLC resonant converter as a wide output range voltage source," *IEEE Trans. Power Electron.*, vol. 27, no. 8, pp. 3749–3763, Aug. 2012.

[16] J. Sun, "Small-signal methods for AC distributed power systems—A review," *IEEE Trans. Power Electron.*, vol. 24, no. 11, pp. 2545–2554, Nov. 2009.

[17] Y. Wang, W. Li, Y. Deng, and X. He, "A novel dual active bridge DC–DC converter with reduced circulating current," *IEEE Trans. Power Electron.*, vol. 31, no. 7, pp. 5060–5070, Jul. 2016.

[18] M. R. Ahmed, R. Todd, and A. J. Forsyth, "Predictive control of bidirectional DC–DC converters in energy storage systems," *IEEE Trans. Ind. Electron.*, vol. 63, no. 6, pp. 3451–3461, Jun. 2016.

[19] Texas Instruments, "Bidirectional CLLLC resonant dual active bridge reference design for HEV/EV onboard chargers," Application Report, 2020.

[20] Z. Fang, J. Wang, and D. Xu, "Soft-switching range extension of dual-active-bridge converters by resonant tank integration," *IEEE Trans. Power Electron.*, vol. 33, no. 2, pp. 1304–1315, Feb. 2018.

[21] Y. Shi, R. Li, and F. C. Lee, "LLL resonant dual active bridge converter with enhanced ZVS capability," *IEEE Trans. Power Electron.*, vol. 34, no. 9, pp. 8653–8665, Sep. 2019.

[22] A. Boglietti, A. Cavagnino, M. Lazzari, and M. Pastorelli, "Thermal analysis of electrical machines and power electronics," *IEEE Trans. Ind. Appl.*, vol. 45, no. 1, pp. 35–44, Jan.–Feb. 2009.

[23] L. Li, G. Xu, D. Sha, Y. Liu, Y. Sun, and M. Su, "Review of dual-active-bridge converters with topological modifications," *IEEE Trans. Power Electron.*, vol. 38, no. 7, pp. 9046–9076, 2023.

[24] P. Ning, F. Wang, and D. Boroyevich, "Thermal-oriented design and optimization of power electronic converters," *IEEE Trans. Power Electron.*, vol. 28, no. 10, pp. 4806–4819, Oct. 2013.

[25] M. Ciappa and W. Fichtner, "," *Microelectron. Reliab.*, vol. 43, no. 9–11, pp. 1653–1658, 2003.

[26] Infineon Technologies, "IKQ50N120CH3 IGBT datasheet," Infineon Technologies AG, 2019.

[27] N. Mohan, T. M. Undeland, and W. P. Robbins, *Power Electronics: Converters, Applications, and Design*, 3rd ed. Hoboken, NJ, USA: Wiley, 2003.
[28] U. Drofenik and J. W. Kolar, "A general scheme for calculating switching- and conduction-losses of power semiconductors," *IEEE Trans. Ind. Electron.*, vol. 55, no. 12, pp. 4196–4207, Dec. 2008.
[29] M. Swetha, K. Susmitha, C. Sairam, V. Venkata Teja, and B. Sravani, "Design and simulation of dual active bridge converter for EV battery charging applications," CRC Press, 2025.

BIOGRAPHIES

Amir Hossein Najaei was born in Tehran, Iran, in 2001. He received the B.S. degree in Electrical Engineering from Tafresh University and the M.S. degree in Power Electronics from Semnan University. His research interests include power electronics, advanced converter topologies, data center power conversion systems, EV/HEV charging systems, and renewable energy integration.

Naser Eskandarian is currently an Assistant Professor in the Faculty of Electrical and Computer Engineering, Semnan University, Semnan, Iran. His research interests include power electronics, advanced DC-DC converters, photovoltaic inverters and MPPT techniques, electric and hybrid electric vehicle (EV/HEV) chargers, renewable energy integration, and robotic control systems.